J. Phys. B: At. Mol. Opt. Phys. **31** (1998) 5361–5368. Printed in the UK PII: S0953-4075(98)96905-X

Isotope effects in the electron impact break-up of water

W Kedzierski, J Derbyshire, C Malone and J W McConkey
Department of Physics, University of Windsor, Windsor, ON, Canada N9B 3P4

Received 20 August 1998

Abstract. Total fragmentation of H_2O and D_2O has been studied as a function of incident energy over the range from threshold to 325 eV. A small subset of possible dissociation channels has been selected by making use of a novel solid xenon matrix detector which is selectively sensitive to $O(^1S)$ metastable atoms. O-fragment kinetic energies and appearance potentials have been measured and significant isotopic effects are observed. Within the errors of the measurements the cross section for $O(^1S)$ production from H_2O is the same as that from D_2O. The cross sections reach a maximum value of 1.5×10^{-18} cm^2 at 100 eV incident electron energy.

1. Introduction

Interest in the dissociation of water has been ongoing for many years, partly because of the importance of such processes in planetary or cometary environments and also because of their relevance to areas such as radiation chemistry.

Early photoabsorption work (Watanabe and Zelikoff 1953), revealed the existence of two broad continua representing the existence of the A and B repulsive states of the parent molecule. These led to the production of ground state H atoms and OH molecules in the $X\,^2\Pi$ and $A^2\Sigma^+$ states, respectively. With the advent of lasers came the pioneering state-specific studies of Andresen *et al* (1984) and others (see Brouard *et al* 1994, for more recent references) which led to a major elucidation of the photodissociation dynamics, at least for the low-lying optically allowed states. Synchrotron radiation studies have also made significant contributions, often by monitoring excited fragment fluorescence or charged fragment production (see, for example, Wu and Judge 1988). Very little optical gas-phase work seems to have involved D_2O or HDO as distinct from H_2O, apart from some seminal work on the first absorption band (Engel *et al* 1988, Engel and Schinke 1988, Shafer *et al* 1989) and the resonance Raman studies of Sension *et al* (1988).

The interaction of photons and charged particles with water and its isotopes in the condensed phase has also been widely studied (see Kimmel and Orlando 1995, 1996, for references). Using resonant enhanced multi-photon ionization (REMPI) techniques they have identified such species as $O(^1D)$ being desorbed from ice surfaces following low-energy electron irradiation.

Fragmentation of water molecules in the gas phase by electron impact has again been largely limited to H_2O targets. Here, production of metastable (Freund 1971, 1983) and non-metastable (Muller *et al* 1992, Trajmar *et al* 1983, McConkey 1984, Kouchi *et al* 1979, Ogawa *et al* 1991) fragments have been studied, as have dissociative ionization and attachment (Mark and Dunn 1985). Both direct and laser induced fluorescence techniques have been applied particularly when production of OH is being monitored (Kawazumi and Ogawa 1987, Darrach

0953-4075/98/245361+08$19.50

and McConkey 1991). In connection with the present work we would like to draw particular attention to the work of Beenakker *et al* (1974) who studied the dissociative excitation process including production of excited O fragments. We also mention the work of Kurawaki *et al* (1983) and Freund (1971) who demonstrated that significant isotope effects occurred in the production of excited H and D from H_2O and D_2O, respectively.

In this work we make use of a novel detector which is selectively sensitive to $O(^1S)$ to study the relative production of this species from H_2O and D_2O targets over the electron energy range from threshold to 325 eV. Pulsed excitation and time-of-flight (TOF) detection allows discrimination between different species produced in the electron impact process. A previous paper (Derbyshire *et al* 1997) has discussed the absolute cross section and dissociation dynamics of D_2O in detail.

2. Experimental

The apparatus has been discussed in detail previously (LeClair and McConkey 1993, 1994) and so only the salient features will be given here. The electron beam crosses the molecular water beam effusing from a capillary tube at right angles. Fragments formed in the interaction drift to a surface detector located 27 cm away in a separate, differentially pumped region. The detector consists of a layer of xenon continuously deposited on a cold finger held at 65–69 K. When $O(^1S)$ atoms impact the Xe surface they thermalize, form XeO excimers and radiate (predominantly a broad band near 725 nm). A cooled photomultiplier with a GaAs photocathode detects the emission through a suitable filter. The electron beam was pulsed and a time-to-amplitude convertor (TAC) was used to acquire TOF spectra at a fixed electron impact energy. Alternatively, TOF windows could be chosen and the electron energy varied under computer control so that excitation functions, appropriate to data arriving at the detector during that window, could be obtained. The detector has very high quantum efficiency for $O(^1S)$ but is completely insensitive to any other species produced in the electron–water interaction.

A crucial factor in the operation of the detector is the temperature of the cold finger. Previous measurements, LeClair and McConkey (1993), on the variation of the sensitivity of the detector with temperature, have been extended down to 65 K and are shown in figure 1. Clearly it is advantageous to work at as low a temperature as possible but, because of the rapid change of sensitivity with temperature, the temperature of the finger had to be carefully controlled when making absolute measurements.

3. Results and discussion

Figure 2 shows TOF data for H_2O and D_2O at an incident electron energy of 90 eV. The large common peaks at short times are due to photons which are generated in the interaction region during the exciting electron pulse and which are scattered into the detector. The centre of this photon peak is taken as the zero of the timescale. As can be seen, a single broad peak is observed with a maximum at a flight time of about 110 (130) μs for D_2O and H_2O respectively. As well as occurring at shorter times, the peak from D_2O is somewhat narrower in half-width (FWHM). As the electron energy is increased above threshold, the leading edges of the TOF peaks are observed to shift slightly to shorter flight times and the FWHM is observed to shrink slightly. There is a hint of a shoulder to the distribution on the short flight-time edge of the peak. The overall structure of the TOF curves and the minor changes which occur as a function of energy suggest that one major process is dominating the $O(^1S)$ production with some minor additional contributions as the energy is increased.

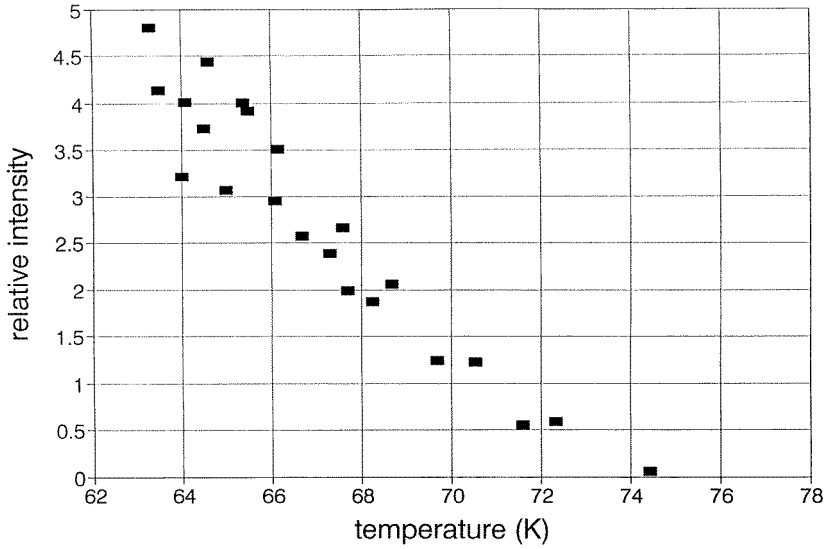

Figure 1. Variation of the metastable signal as a function of the temperature of the cold finger. The electron energy is 100 eV and a CO_2 target is used. The data represent many measurements taken over an extended time period. (See text for further details).

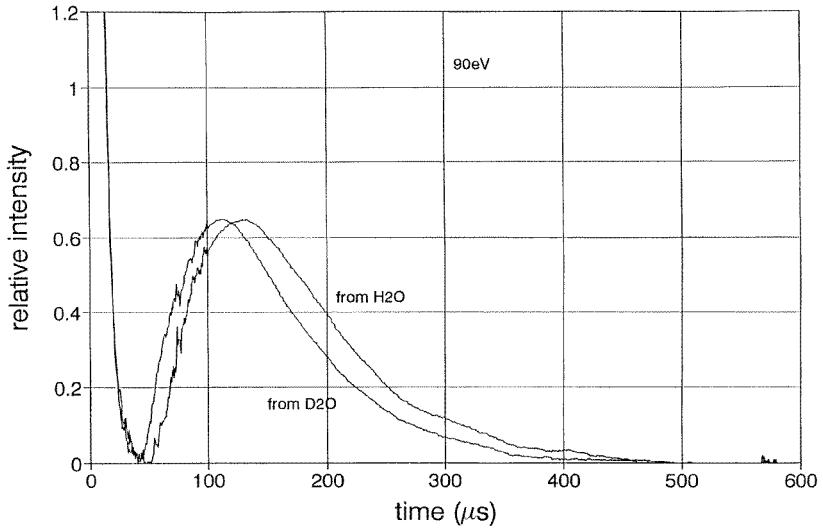

Figure 2. TOF spectra for metastable $O(^1S)$ fragments produced by 90 eV electron impact on H_2O and D_2O. Zero time corresponds to the centre of the 20 μs wide electron pulse. The spectra have been normalized so that the metastable peaks are the same height.

The differences between the data from the two targets simply reflects the fact that, although the repulsive curves and hence the total released kinetic energy for the two molecules must be the same, the sharing of the released kinetic energy between the different fragments depends on their respective masses. For example, simple momentum considerations show that if two fragment break-up was occurring into $O + H_2(D_2)$, then the ratio of the O TOFs from the two targets should be 1.34. The fact that it is somewhat less than this (figure 2), reflects the fact

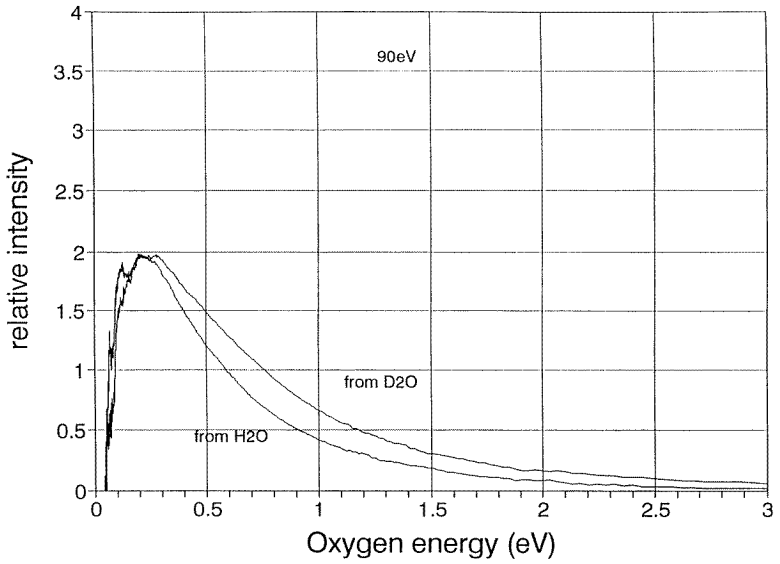

Figure 3. O(^{1}S) fragment kinetic energy spectra obtained from the data of figure 2. The spectra have been normalized so that the peaks are the same height.

that the break-up is more complicated (three-fragment rather than two-fragment, see later) and also the fact that some blurring is occurring due to the directed motion of the target molecules.

Because the mass of the detected particle is known, it is trivial to convert the TOF data to kinetic energy spectra (see LeClair and McConkey 1993, for details). This is illustrated in figure 3. Clearly a single peak is obtained for each target with a long tail extending to higher energies. The D_2O peak is significantly broader and the maximum occurs at a slightly higher energy, 0.25 compared to 0.2 eV, than in H_2O. As the electron impact energy is reduced, the widths of the fragment energy peaks are observed to get smaller and the positions of the maxima move to lower energies. For example, with D_2O targets the position of the maximum occurs at 0.15 eV when the impact energy is reduced to 30 eV. All of this supports the suggestion made above that additional production channels open up as the incident electron energy is increased. The long tails to the kinetic energy distributions suggest that the repulsive surfaces rise steeply towards the inner edge of the Franck–Condon region.

We note that the accuracy in the process of converting TOF to kinetic energy data is reduced at the lowest energies (longest flight times) due to the small signals and the t^3 factor which is involved. Kinematic effects could also occur at energies close to the thermal energy (25 meV) of the parent beam. For these reasons data at the very lowest energies have been suppressed.

An excitation function for production of O(^{1}S) from either of the two targets is shown in figure 4. The energy scale was calibrated using the threshold for production of prompt photons (mainly Balmer-α, Beenakker *et al* 1974). Both curves are observed to rise from a threshold around 15.5 eV to a broad maximum near 100 eV. Such an excitation function shape is characteristic of optically allowed transitions in the parent molecule. Within the accuracy of the measurements the H_2O and D_2O data are indistinguishable.

The cross section data of figure 4 were made absolute using a modified relative flow technique (Trajmar *et al* 1996). The signals were compared with those obtained from CO_2 under the same conditions of excitation (electron beam energy (100 eV) and current, target gas

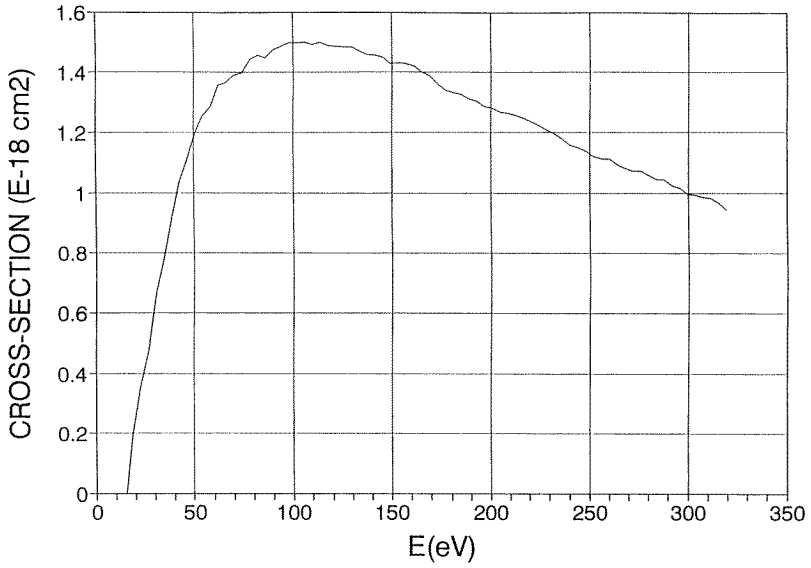

Figure 4. Absolute cross section for production of $O(^1S)$ from H_2O or D_2O as a function of impact electron energy. Some smoothing has been applied to reduce the statistical scatter in the data. (See text for details of calibration procedure.)

density etc). Isotropic emission of fragments from both molecules was assumed. A CO_2 cross section of 1.56×10^{-17} cm^2 at 100 eV was used for normalization (LeClair and McConkey 1994). In addition to providing the calibration standard, the signal obtained from CO_2 was used to continuously monitor the sensitivity of the xenon matrix surface. A calibration spectrum was accumulated before and after each data run with water targets. By keeping all other experimental parameters the same, the CO_2 signal automatically provided a sensitivity check. Variations of the order of 10% were often observed, probably due to changes in the thickness and hence the surface temperature of the Xe layer with time.

It was very important to make the comparison between water and CO_2 under the same conditions of electron beam current and target gas density. The electron beam current was carefully monitored and controlled and the following procedure was used to obtain relative target densities. Because of the different molecular masses and hence molecular speeds, and because, for reasons of obtaining sufficient signal, we were operating in a pressure range outside of the molecular flow region, it was not sufficient to make comparisons under conditions where the head pressures behind the capillary inlet tube were the same. An initial experiment was carried out in which the intensities of the prompt photons due to dissociative excitation of the target molecules were monitored as a function of the head pressure behind the capillary. This is shown in figure 5. Initially, at very low pressures, where molecular flow occurs, the curves are linear and the slopes have been normalized in this region. As the head pressure is raised the curves diverge with the CO_2 curve rising more rapidly. This indicates that the target CO_2 density in the interaction region was higher than the H_2O density, for the same head pressure. Since these photon signals were not affected by such phenomena as trapping of resonance radiation (fragment densities were just too small), they could be taken as a direct measure of the relative target density. Thus, measured signals could be readily and accurately corrected.

Other sources of uncertainty in the calibration procedure arose because of the difficulty of maintaining constant experimental parameters over the long (24 h) data taking periods when

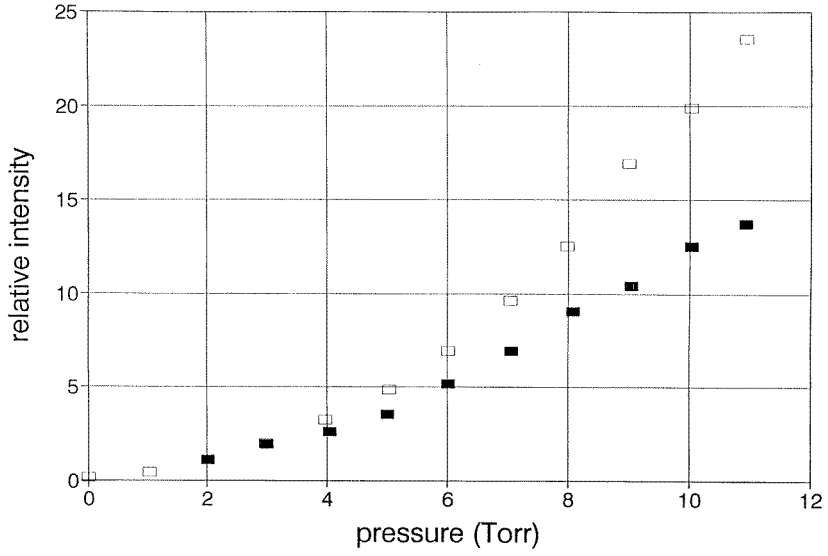

Figure 5. Graph showing the variation of prompt photon signal with head pressure for H_2O and CO_2 (lower and upper data sets, respectively). The electron energy is 100 eV in each case. (See text for further details.)

water targets were being used. In addition, it was assumed that the sensitivity of the detector was independent of the impinging O-atom speed. Since thermalization of the $O(^1S)$ atoms occurs prior to excimer formation and since the range of fragment speeds is similar for water and CO_2, this assumption is judged to be reasonable. A large number of calibration runs were carried out using both targets and averaged to obtain the final result which is given in figure 4. A broad maximum in the excitation function occurs close to 100 eV. Its value there is 1.5×10^{-18} cm^2. An overall uncertainty in this figure of 30% is estimated including a quoted uncertainty of 12% in the calibration standard. We note that this value is slightly greater than the number given by Derbyshire *et al* (1997). This is because a significantly larger data base has now been obtained and a rather better control of gas beam densities has been achieved.

The measured appearance energy was 15.5 ± 1.0 eV. Thus, assuming that the maximum in the kinetic energy spectrum, figure 3, results from a vertical transition in the centre of the Franck–Condon region, and assuming an average total energy release (based on momentum considerations) of 1.5–2.5 eV, allows us to estimate the energy at infinite separation from the measured appearance energy to be in the range 12–15 eV. The only possible fragmentation process which fits these parameters is

$$e + H_2O(X\,^1A_1) \rightarrow H_2O^*(^1A_1) \rightarrow O(^1S) + 2H(^2S)$$

with a threshold energy at infinite separation of 13.696 eV (13.82 eV in D_2O). If one of the H-atoms was excited, the threshold would be at least 10.2 eV higher in energy. Similarly, if the two H atoms were united as a molecule the threshold energies would be 9.177 eV for $H_2(X, v = 0)$, 20.36 for $H_2(B, v = 0)$ or higher for other possibilities. Clearly these channels can also be excluded as possibilities. We note that Theodorakopoulos *et al* (1982) have carried out *ab initio* calculations of H_2O dissociation into H_2 and an oxygen fragment. Their work reveals that a significant barrier (4 eV) exists towards dissociation into $O(^1S)$ and $H_2(X)$. This would increase the threshold energy for this channel of dissociation to approximately 13.2 eV. However, this is still some 2 eV less than what we measure.

Knowing the identities of the dissociation fragments and knowing, from the shape of the excitation function (figure 4), that spin exchange does not occur in the excitation process leading to the parent repulsive state, allows the state to be unambiguously assigned using the procedure given by Herzberg (1967), as $^1A_1$. It is not possible to identify the other channels, mentioned earlier, which open up at higher energies. Clearly the parent states have zero spin or sharp structure would show up on the excitation function (figure 4). A slight shoulder is observed on the excitation functions about 10 eV above threshold. This is consistent with total fragmentation of the parent molecule with excitation of one of the H atoms to the $n = 2$ state. This conjecture is consistent with the work of various groups who have noted a threshold for $H(n = 2)$ production near 25 eV in the dissociative excitation of water by electron impact, (McGowan *et al* 1969, Bose and Sroka 1971, 1973, Morgan and Mentall 1974, Mohlmann *et al* 1978).

At 100 eV the cross section for Lyman-α production from e-impact on H_2O was measured to be 19.2×10^{-18} cm^2 (Mohlmann *et al* 1978). More recent developments (see Woolsey *et al* 1986) in calibration standards in the VUV spectral region suggest that this number should be revised downwards by a factor of 0.59 to 11.4×10^{-18} cm^2. Combining this with the data of Beenakker *et al* (1974), suggests that the total dissociative excitation cross section of H_2O at 100 eV with production of excited fragments, other than $O(^1S)$, is approximately 16.5×10^{-18} cm^2. Thus $O(^1S)$ production accounts for about 8% of H_2O dissociation which leads to excited neutral fragments. This is a small but not an insignificant dissociation channel. Wu and Judge (1988) studied the absorption of water leading to neutral fragments and show minor structure on their curves near 79.9 nm (15.5 eV). This would be consistent with the opening of the $O(^1S)$ channel observed here.

4. Conclusions

Measurements of TOF and kinetic energy spectra following dissociative excitation of water have revealed significant isotope effects. These may be explained in terms of Franck–Condon excitation of repulsive curves followed by total fragmentation of the molecule. Relative velocities of the various fragments are then governed by the dissociation dynamics and simple momentum considerations. The first repulsive curve leading to $O(^1S)$ also produces two ground state H atoms. It is $^1A_1$ in character. Other channels which contribute to $O(^1S)$ production at higher energies are also optically allowed from the ground state. The cross sections for production of $O(^1S)$ from H_2O and D_2O targets are the same, within the errors of the measurements.

Acknowledgments

We are grateful to the Natural Sciences and Engineering Research Council of Canada for financial assistance and to the staff of the mechanical and electronic workshops at the University of Windsor for expert technical assistance.

References

Andresen P, Ondrey G S, Titze B and Rothe E W 1984 *J. Chem. Phys.* **80** 2548
Beenakker C I M, De Heer F J, Krop H B and Mohlmann G R 1974 *J. Chem. Phys.* **6** 445
Bose N and Sroka W Z 1971 *Z. Naturf.* a **26** 1491
——1973 *Z. Naturf.* a **28** 22
Brouard M, Langford S R and Manolopoulos D E 1994 *J. Chem. Phys.* **101** 7458

Darrach M and McConkey J W 1991 *Chem. Phys. Lett.* **184** 141
Derbyshire J, Kedzierski W and McConkey J W 1997 *Phys. Rev. Lett.* **79** 2229
Engel V and Schinke R 1988 *J. Chem. Phys.* **88** 6831
Engel V, Schinke R and Staemmler V 1988 *J. Chem. Phys.* **88** 129
Freund R S 1971 *Chem. Phys. Lett.* **9** 135
——1983 *Rydberg States of Atoms and Molecules* ed R F Stebbings and F B Dunning (Cambridge: Cambridge University Press)
Herzberg G 1967 *Molecular Spectra and Molecular Structure* vol III (Princeton, NJ: Van Nostrand)
Kawazumi H and Ogawa T 1987 *Chem. Phys.* **114** 149
Kimmel G A and Orlando T M 1995 *Phys. Rev. Lett.* **75** 2606
——1996 *Phys. Rev. Lett.* **77** 3983
Kouchi N, Ito K, Hatano Y, Oda N and Tsuboi T 1979 *Chem. Phys.* **36** 239
Kurawaki J, Ueki K, Higo M and Ogawa T 1983 *J. Chem. Phys.* **78** 3071
Le Clair L R and McConkey J W 1993 *J. Chem. Phys.* **99** 4566
——1994 *J. Phys. B: At. Mol. Opt. Phys.* **27** 4039
Mark T D and Dunn G H 1985 *Electron Impact Ionization* (Berlin: Springer)
McConkey J W 1984 *Argonne National Laboratory Report* ANL 84-28, p 129
McGowan J W, Williams J F and Vroom D A 1969 *Chem. Phys. Lett.* **3** 614
Mohlmann G R, Shima K H and De Heer F J 1978 *Chem. Phys.* **28** 331
Morgan H D and Mentall J E 1974 *J. Chem. Phys.* **60** 4734
Muller U, Bubel Th and Schulz G 1992 *Z. Phys.* D **25** 167
Ogawa T, Yonekura N, Tsukada M, Ihara S, Yasuda T, Tomura H, Nakashima K and Kawazumi H 1991 *J. Phys. Chem.* **95** 2788
Sension R M, Brudzynski R M and Hudson B S 1988 *Phys. Rev. Lett.* **61** 694
Shafer N, Satyapal S and Bersohn R 1989 *J. Chem. Phys.* **90** 6807
Theodorakopoulos G, Nicolaides C A, Buenker R J and Peyerimhof S D 1982 *Chem. Phys. Lett.* **89** 164
Trajmar S, McConkey J W and Kanik I 1996 *At. Mol. Opt. Phys. Handbook* ed G W F Drake (New York: AIP)
Trajmar S, Register D F and Chutjian A 1983 *Phys. Rev.* **97** 219
Watanabe K and Zelikoff M 1953 *J. Opt. Soc. Am.* **43** 753
Woolsey J M, Forand J L and McConkey J W 1986 *J. Phys. B: At. Mol. Phys.* **19** L493
Wu C Y R and Judge D L 1988 *J. Chem. Phys.* **89** 6275